



## Short communication

Influences of Alq<sub>3</sub> as electron extraction layer instead of Ca on the photo-stability of organic solar cellsZhiyong Liu<sup>a,\*</sup>, Miaomiao Tian<sup>b,c</sup>, Ning Wang<sup>d</sup><sup>a</sup> School of Physics and Electronic Science, Changsha University of Science and Technology, Changsha 410004, People's Republic of China<sup>b</sup> College of Physics, Changchun Normal University, 677 North Changji Road, Changchun 130032, People's Republic of China<sup>c</sup> State Key Laboratory of Polymer Physics and Chemistry, Changchun Institute of Applied Chemistry, Chinese Academy of Sciences, Renmin Street, 5625, Changchun 130022, People's Republic of China<sup>d</sup> Changchun Institute of Applied Chemistry, Chinese Academy of Sciences, 5625 Renmin Street, Changchun 130022, People's Republic of China

## H I G H L I G H T S

- We have successfully introduced Alq<sub>3</sub> as electron extraction layer (EEL) for PSCs.
- The device performance based on Alq<sub>3</sub> is fully comparable to those based on Ca.
- The PSCs with Alq<sub>3</sub> as EEL presented superior photo-stability than that with Ca as EEL.
- Alq<sub>3</sub> is an alternative candidate for high-performance and photo-stability polymer solar cells.

## A R T I C L E I N F O

## Article history:

Received 10 September 2013

Received in revised form

17 October 2013

Accepted 24 October 2013

Available online 12 November 2013

## Keywords:

Electron extraction layer

Stability

Power conversion efficiency

Polymer solar cell

## A B S T R A C T

Calcium (Ca) is not a desirable candidate as electron extraction layer (EEL) for long-term stability organic photovoltaics (OPVs) on account of its nature of active metal. In this paper, we have selected thieno[3,4-b]thiophene/benzodithiophene (PTB7) and [6,6]-phenyl C71-butyric acid methyl ester (PC<sub>71</sub>BM) as donor and acceptor, respectively, and the device architecture is Glass/ITO/poly(ethylenedioxythiophene):polystyrene sulphonate (PEDOT:PSS)/PTB7:PC<sub>71</sub>BM/EEL/Aluminum. For comparison, tris (8-hydroxyquinoline) aluminum (Alq<sub>3</sub>) and Ca were used as EEL to reveal their influence on the performance [power conversion efficiency (PCE), short-circuit current density (*J*<sub>sc</sub>), open-circuit voltage (*V*<sub>oc</sub>) and fill factor (FF)] of the OPVs. As a result, PCE of the device with Ca as EEL rapidly reduced over 60% after three days due to the poor stability of Ca. The device with Alq<sub>3</sub> as EEL shows favorable stability owing to the PCE moderate declined less than 30% after one month. Furthermore, PCE of the device with Alq<sub>3</sub> as EEL was fully comparable to that with Ca as EEL. Our results indicate that Alq<sub>3</sub> is an alternative candidate for high-performance and long-term photo-stability OPVs.

© 2013 Elsevier B.V. All rights reserved.

## 1. Introduction

Significant progress has been made over the past 25 years in improving efficiency for organic photovoltaics (OPVs) [1,2]. And with good reason, the inexpensive materials and roll-to-roll processes involved in this technology could potentially allow a massive production of cost effective, flexible, and large scale polymer solar cells [3–5]. As a result of the successful device architecture of bulk heterojunction, performance of OPVs increased continuously when

using poly (3-hexylthiophene) (P3HT) and phenyl-C61-butyric acid methyl ester (PCBM) blend as photoactive layer [6]. Moreover, benefiting from the introduction of low band-gap conjugated polymer which extends the harvesting of the solar spectrum beyond 650 nm, the bottleneck of PCEs of OPVs could be overcome [2,5,7]. However, at the outset efficiencies beyond 6% have only been achieved when fine tuning of electrical material properties, optimized architectural device construction and extended the harvesting of the solar spectrum have been implemented. Hou et al. developed a new low band-gap polymer, poly[4,8-bis-(2-ethyl-hexyl-thiophene-5-yl)-benzo[1,2-b:4,5-b']dithiophene-2,6-diyl]-alt-[2-(2'-ethyl-hexanoyl)-thieno[3,4-b]thiophen-4,6-diyl] (PBDTTT-C-T), 7% and 8% efficiencies were achieved in traditional and inverted device constructions, respectively [8]. The 9% barrier

\* Corresponding author.

E-mail addresses: [zhylu2006@163.com](mailto:zhylu2006@163.com) (Z. Liu), [tmm8066@163.com](mailto:tmm8066@163.com) (M. Tian), [ning\\_wang@outlook.com](mailto:ning_wang@outlook.com) (N. Wang).

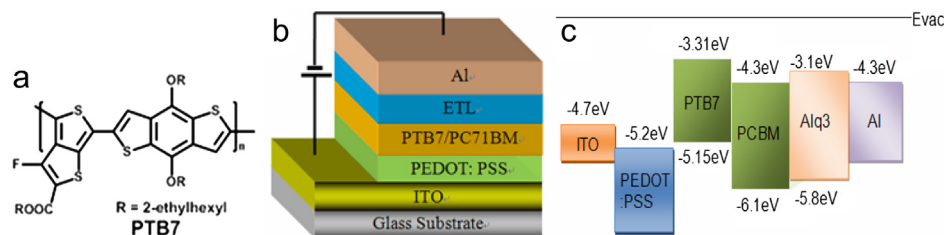


**Fig. 1.** Device architecture and energy level diagram of the polymer solar cell. a) Chemical structures of PTB7. b) Schematic of the polymer solar cell. c) Energy level diagram of the device.

was broken in 2012 when Cao et al. used new interfacial materials to improve the performance of OPVs with PTB7/PC<sub>71</sub>BM as active layer [9]. Very recently, Yang group overfulfilled 10% PCE by successfully employing an inverted tandem architecture [10].

Even though the low band gap based cells are promising in terms of the rapidly improvement of PCEs. The photo-stability of low band gap based devices in atmospheric condition still remains an unsolved problem, and it represents a major hurdle before the upscale productions. While efficiencies are steadily improved, the stability of organic solar cells has limited the application of OPVs [11–13]. The power conversion efficiencies of OPVs have attracted

much attention of many groups, however, the photo-stability of OPVs has only a small amount of papers [14–16]. So investigation on photo-stability is very necessary for OPVs to meet the commercial requirements.

The device geometry of typical laboratory-scale OPVs is composed of a transparent indium tin oxide (ITO) anode, a hole-extracting interfacial layer-PEDOT:PSS, a photoactive layer, electron-extracting layer and a low work-function metal cathode [17,18]. Generally, lithium fluoride (LiF) and Ca are used as cathode interfacial layer [19,20]. The thickness demand for LiF film is very rigorous and PCEs of solar cells can be tremendously affected when the thickness of LiF is extremely thin or excessively thick. So the thickness of LiF is neither thin nor thick [21–23]. Chemical property of Ca is active and easily oxidized by oxygen and water [24,25]. The development of new EEL materials that have low dependency to variations in thickness is therefore a key step for the development of OPVs with significantly increased photo-stability [26]. Alq<sub>3</sub> is a small molecular and can be easily deposited by vacuum evaporation. Moreover, high electron mobility of Alq<sub>3</sub> thin film within tens of nanometers has confirmed [27,28]. Combining with appropriate values of highest occupied molecular orbital (HOMO) and lowest unoccupied molecular orbital (LUMO), Alq<sub>3</sub> is a potential EEL material for photo-stability OPVs. Herein, we have successfully introduced Alq<sub>3</sub> as EEL for polymer solar cells. The influences of Alq<sub>3</sub> on the performance (photo-stability, PCE,  $V_{OC}$ ,  $J_{SC}$ , FF) of solar cells were carried out in detail.

## 2. Experimental

### 2.1. Materials

PTB7 and PC<sub>71</sub>BM were purchased from 1-material Inc. and Sigma–Aldrich Co, respectively. PEDOT:PSS (Clevios P V Al4083) was purchased from HC Starck. *o*-Dichlorobenzene (ODCB, anhydrous, 99%) was purchased from Sigma–Aldrich Co. Alq<sub>3</sub> was purchased from Luminescence Technology Co. Ca and Al were purchased from Alfa Aesar Co.

### 2.2. Device preparation and characteristics

PTB7/PC<sub>71</sub>BM (1:1.5, wt%) blends were dissolved in ODCB solution overnight with PTB7 concentration of 10 mg ml<sup>-1</sup>. About 3%

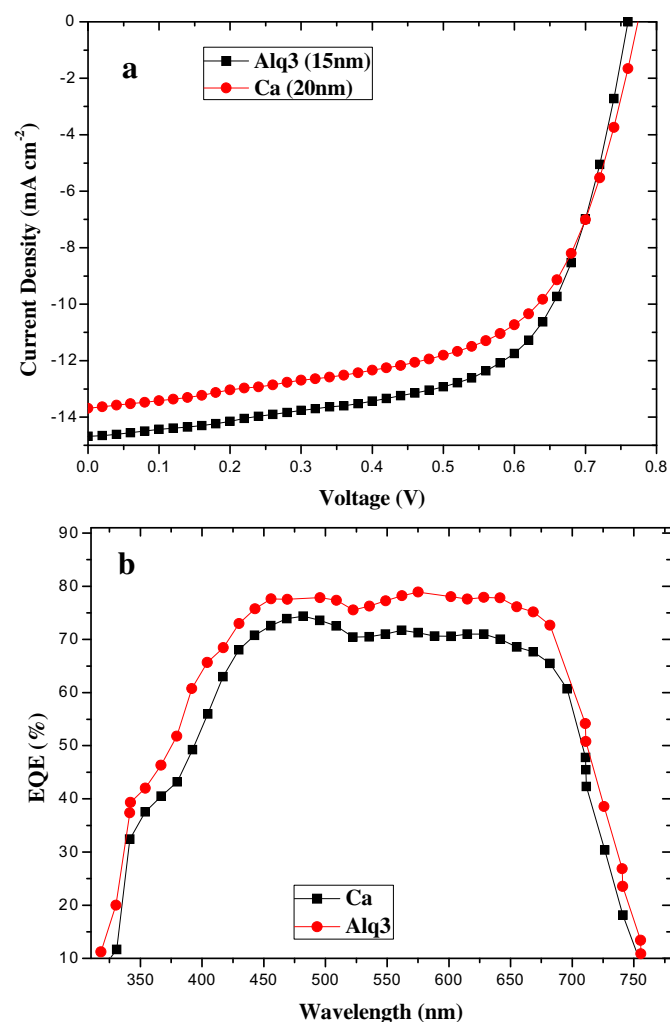


**Fig. 2.** a) Current density–voltage characteristics of the OPVs under 100 mW cm<sup>-2</sup> AM 1.5G illumination based on Alq<sub>3</sub> and Ca as EELs, respectively. b) Corresponding external quantum efficiency curves for a).

**Table 1**  
Device characteristic parameters of the optimized OPV devices with different Alq<sub>3</sub> thickness and Ca acted as the ETL materials.

EEL thickness (nm)	Alq <sub>3</sub> (5 nm)	Alq <sub>3</sub> (10 nm)	Alq <sub>3</sub> (15 nm)	Alq <sub>3</sub> (20 nm)	Alq <sub>3</sub> (25 nm)	Ca (20 nm)
$V_{OC}$ (V)	0.68	0.7	0.76	0.75	0.62	0.77
$J_{SC}$ (mA cm <sup>-2</sup> )	8.8	10.5	13.2	10.9	10.2	13.2
FF (%)	56	60	64	62	52	62
PCE (%)	3.4	4.4	6.4	5.1	3.3	6.3

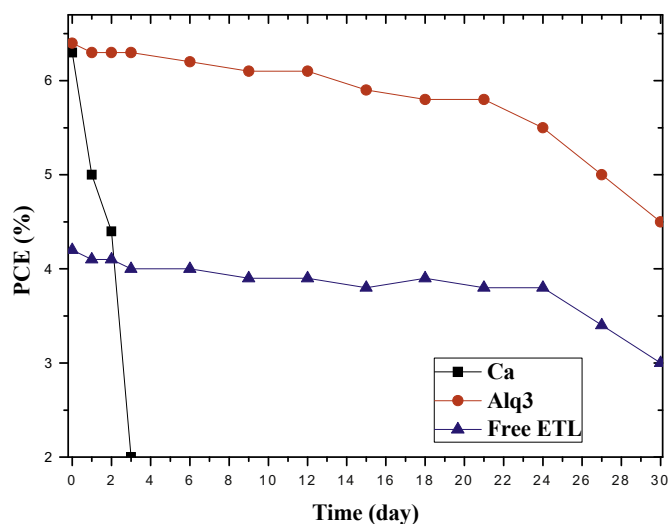


**Fig. 3.** Photo-stability characteristics of the un-encapsulated OPVs with Alq<sub>3</sub> and Ca as EEL and without EEL in glove box for one month.

(1,8-diiodooctane (DIO)/1,2-dichlorobenzene (DCB), v/v) of DIO as an additive is helpful to obtain better photovoltaic results. The ITO substrates were ultrasonicated in 30 °C aqueous detergent followed by isopropyl alcohol, acetone and deionized water for 30 min each. The substrates were dried under a stream of nitrogen and heating of hot-stage. UV/ozone treatment of ITO glass for 20 min. First, a 30-nm-thick PEDOT:PSS anode buffer layer was spin-cast on the ITO substrate, and subsequent baking at 130 °C for 10 min in air. The PTB7:PC<sub>71</sub>BM active blend layer has a nominal thickness of ~90 nm

(with a variation of ~15 nm over the entire film). The Alq<sub>3</sub>, Ca layers and Al cathode were vacuum evaporated through a shadow mask to define the active area of the devices (10 mm<sup>2</sup>). The thickness for Al and Ca are 150 and 20 nm, respectively, and the thickness of Alq<sub>3</sub> is various according to the experiment requests. The *J*–*V* characteristics and lifetime of OPV were performed in a glove box under illumination at 100 mW cm<sup>−2</sup> using an AM 1.5G solar simulator. The chemical structure PTB7, schematic diagram of proposed OPV, and energy level diagram of device are shown in Fig. 1.

### 3. Results and discussion

As shown in Fig. 2a, current density–voltage (*J*–*V*) curves of OPVs with optimized Alq<sub>3</sub> and Ca thickness that act as EEL layer are presented. In our experiments all *J*–*V* measurements were performed under illumination from a 150 W solar simulator with AM 1.5G filters with the intensity of 100 mW cm<sup>−2</sup> and the device characteristic parameters under different Alq<sub>3</sub> thickness are shown in Table 1. With an Alq<sub>3</sub> thickness of 5 nm for device, a PCE of 3.4% with a short circuit current density (*J*<sub>SC</sub>) of 8.8 mA cm<sup>−2</sup>, an open circuit voltage (*V*<sub>OC</sub>) of 0.68 V, and an FF of 56% was achieved. When the Alq<sub>3</sub> layer thickness was increased to 10 nm the PCE of device reached 4.4%, with a *J*<sub>SC</sub> of 10.5 mA cm<sup>−2</sup>, a *V*<sub>OC</sub> of 0.7 V, and an FF of 60%. In the case of the Alq<sub>3</sub> layer thickness was 15 nm, the optimized PCE of 6.4% was accomplished with a *V*<sub>OC</sub> of 0.76 V, a *J*<sub>SC</sub> of 13.2 mA cm<sup>−2</sup>, and an FF of 64%. However, the PCE of OPV decreased while the thickness of Alq<sub>3</sub> increased. When the Alq<sub>3</sub> layer thickness attained 25 nm, the efficiency was dropped to 3.3%, with a *J*<sub>SC</sub> of 10.2 mA cm<sup>−2</sup>, a *V*<sub>OC</sub> of 0.62 V, and an FF of 52%. For comparison, the devices with Ca as EEL material were fabricated and the

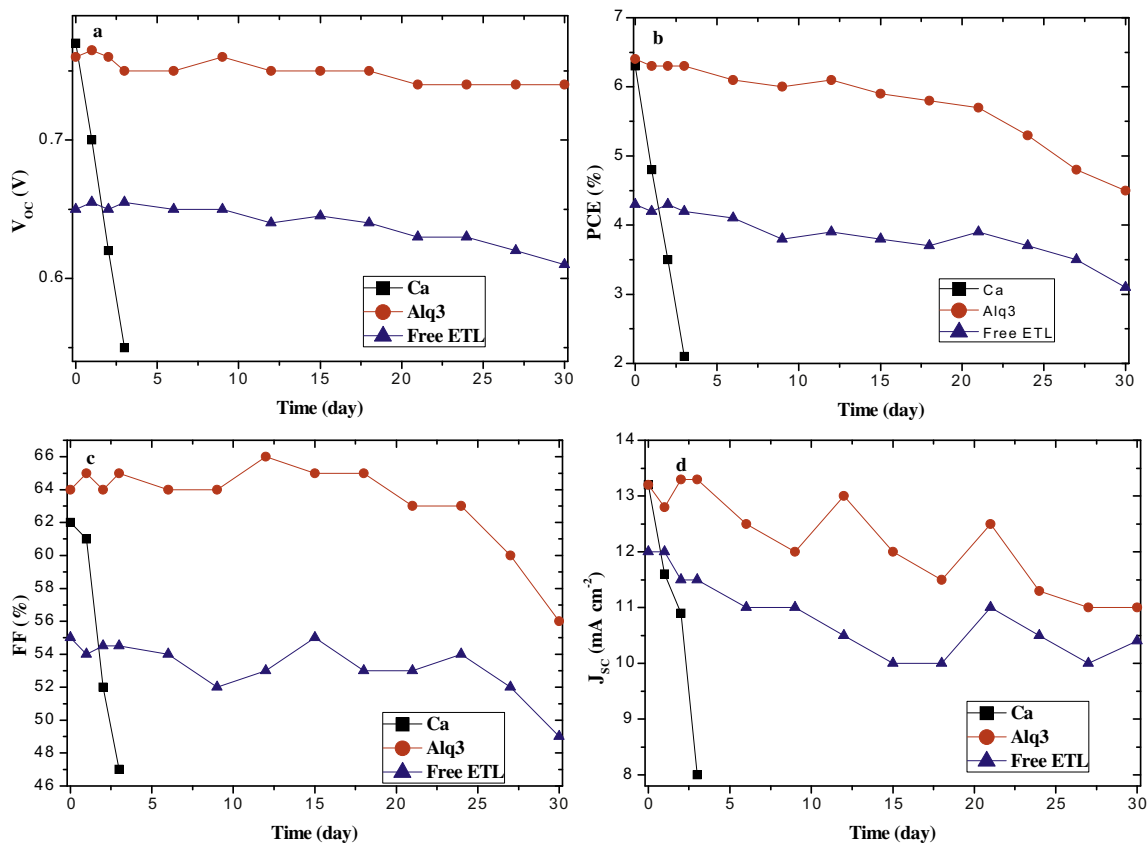


**Fig. 4.** Characteristic parameters of decay rate for the OPVs with different EELs: a) open-circuit voltage; b) power conversion efficiency; c) fill factor; d) short-circuit current density.

optimized performance was carried out with a PCE value of 6.3% ( $J_{SC} = 13.2 \text{ mA cm}^{-2}$ ,  $FF = 62\%$ ,  $V_{OC} = 0.77 \text{ V}$ ). These results are moderate lower than those based on optimized  $\text{Alq}_3$  thickness. As an organic small molecular material, the organic–organic interface between  $\text{Alq}_3$  and photoactive layer may be more favorable to charge transport in comparison with the organic–metal case. Secondly, the electron mobility of  $\text{Alq}_3$  is approximately within  $10^{-3}$ – $10^{-4} \text{ cm}^2 \text{ V}^{-1} \text{ s}^{-1}$  order of magnitude due to the existence of Al, which is desired for ideal electron extracting layer in polymer solar cells because of the reported high efficient conjugated polymers usually possess an electron mobility  $\sim 10^{-3} \text{ cm}^2 \text{ V}^{-1} \text{ s}^{-1}$ . Such substantial mobility value of  $\text{Alq}_3$  should partially account for fill factor and short-circuit current density, although the mobility alone cannot guarantee high device performance. Our results demonstrate that  $\text{Alq}_3$  is an alternative EEL material for high-performance OPVs. Fig. 2b shows the external quantum efficiency (EQE) curves of devices based on various EEL materials. It was identified that the  $J_{SC}$  measured from devices were in good agreement with integrated values of the EQE spectrum.

The LUMO level of EEL is lower than that of PCBM and Al that would cause a large barrier for electron to reach the cathode. Although the LUMO level of  $\text{Alq}_3$  is not fully matched with the adjacent layers, electron transport can occur through damage-induced trap states created by the evaporation of hot metal atoms onto the  $\text{Alq}_3$  surface [29,30]. Owing to the metallic nature of Ca and ohmic contact between the active layer and electrode, however,  $\text{Alq}_3$  cannot create ohmic contact between the active layer and electrode [31]. When the  $\text{Alq}_3$  layers are less than 15 nm thick and the adjoining layers are deposited under controlled conditions, effective electron channels thereby formed are stable and the charge carrier transport process is not affected [32]. Therefore, while the thickness of  $\text{Alq}_3$  is higher than 15 nm, the electron transport and charge carrier collection process will be affected by the large barrier between the active layer and metal electrode. Moreover,  $\text{Alq}_3$  has superior stability in organic light emitting diode [33,34]. It is considerably necessary to explore the lifetime behavior of OPVs with  $\text{Alq}_3$  as EEL material for them to be brought to market as quickly as possible.

The photo-stability of un-encapsulated PTB7:PC<sub>71</sub>BM polymer solar cells as a function of storage time in glove box ambient condition under illumination with  $\text{Alq}_3$  and Ca as EEL material was studied. Meanwhile, the solar cells without EEL were also prepared for comparison with above mentioned devices. Fig. 3 exhibits the PCE values as a function of storage time. Under continuous illumination for 30 days all PCE values dropped with storage time. Obviously, the PCE values of device with Ca as EEL material sharply declined within 3 days and it dropped over 60% of the initial PCE value. Taking into account the fact of Ca is active metal and trace amounts oxygen and water (<0.1 ppm) are being in glove box, the photo-stability of device will be affected tremendously by Ca. Comparing with previous work by M. Tavakkoli et al., the device with Ca as EEL has a higher decay rate of PCE than the OPV with LiF as buffer layer [35,36]. In contrast, the degradation rate of OPVs with  $\text{Alq}_3$  as EEL and without EEL showed slow descending tendency. The device without EEL material showed a moderate decrease in PCE less than 30% of its initial value. Voroshazi et al. had studied the degradation behavior of P3HT:PCBM solar cells with a PEDOT:PSS buffer layer, which showed a similar attenuation process under  $\text{N}_2$  inert atmosphere [37]. Apart from the fact that acidic PEDOT:PSS can etch ITO anode, the reaction of PSS with the blend components of photoactive layer was proposed as another possible reason for the performance degradation. These shortcomings directly affect the ability of charge carriers of ITO anode [11,38]. In the case of  $\text{Alq}_3$  as EEL, the curve of PCE versus storage time showed similar tendency with the curve of device without EEL. The

performance degradation of device mainly derived from the influence of PEDOT:PSS in the long-term measurement. Furthermore, the metal Ca atom may diffuse into adjacent photoactive layer during thermal evaporating, which will extremely cause device degradation. On the contrary, this problem can be effectually circumvented by organic/organic contact in the case of  $\text{Alq}_3$ /photoactive layer. These results indicate that the  $\text{Alq}_3$  EEL is an alternative material for long-term photo-stability OPVs.

All device characteristic parameters of degradation rate with different EEL materials are shown in Fig. 4. As shown in Fig. 4, the three device characteristic parameters ( $J_{SC}$ , FF and PCE) of device with Ca as EEL decrease sharply (the degradation rates dropped more than 30% of its initial value), only  $V_{OC}$  has decreased moderately (the degradation rates dropped less than 30% of its initial value). The  $V_{OC}$  of device with  $\text{Alq}_3$  as EEL and without EEL did not obviously change and the other three devices characteristic parameters ( $J_{SC}$ , FF, and PCE) showed almost identical trends. Due to the  $V_{OC}$  is associated with the difference between LUMO level of acceptor and HOMO level of donor, it can only be affected slightly in device with storage time [39,40]. The other parameters ( $J_{SC}$  and FF) are closely linked to the morphology of photoactive layer and interfaces between active layer and charge extraction layers. Thus,  $J_{SC}$ , FF and PCE have a faster decay rate than  $V_{OC}$  within one month.

#### 4. Conclusion

We have studied the photo-stability behavior of OPVs with  $\text{Alq}_3$  as EEL under continuous illumination. The performance of devices with  $\text{Alq}_3$  as EEL is fully comparable to that with Ca as EEL under illumination of AM 1.5G, 100  $\text{mW cm}^{-2}$ . Moreover, the device with  $\text{Alq}_3$  as EEL has great advantage in photo stability than that with Ca as the EEL. Long-term photo-stability of the un-encapsulated OPVs based on PTB7:PC<sub>71</sub>BM was improved by using 15 nm thick  $\text{Alq}_3$  EEL instead of Ca. Our work gives an effective method in accomplishing efficient and high photo-stability OPVs.

#### Acknowledgments

This work was financially supported by the National Natural Science Foundation of China (NSFC, grant no. 21104077).

#### References

- [1] R. Zhu, A. Kumar, Y. Yang, *Adv. Mater.* 23 (2011) 4193–4198.
- [2] E. Bundgaard, F.C. Krebs, *Sol. Energy Mater. Sol. Cells* 91 (2007) 954–985.
- [3] B.A. Bailey, M.O. Reese, D.C. Olson, S.E. Shaheen, N. Kopidakis, *Org. Electron.* 12 (2011) 108–112.
- [4] G.H. Jung, K. Hong, W.J. Dong, S. Kim, J.-L. Lee, *Adv. Energy Mater.* 1 (2011) 1023–1028.
- [5] G.D. Sharma, P. Balraju, J.A. Mikroyannidis, M.M. Stylianakis, *Sol. Energy Mater. Sol. Cells* 93 (2009) 2025–2028.
- [6] Y. Liang, D. Feng, Y. Wu, S.-T. Tsai, G. Li, C. Ray, L. Yu, *J. Am. Chem. Soc.* 131 (2009) 7792–7799.
- [7] J.A. Mikroyannidis, D.V. Tsakournos, S.S. Sharma, Y.K. Vijay, G.D. Sharma, *J. Mater. Chem.* 21 (2011) 4679–4688.
- [8] L. Huo, S. Zhang, X. Guo, F. Xu, Y. Li, J. Hou, *Angew. Chem.* 50 (2011) 9697–9702.
- [9] Z. He, C. Zhong, S. Su, M. Xu, H. Wu, Y. Cao, *Nat. Photon.* 6 (2012) 591–595.
- [10] J. You, L. Dou, K. Yoshimura, T. Kato, K. Ohya, T. Moriarty, K. Emery, C.-C. Chen, J. Gao, G. Li, Y. Yang, *Nat. Commun.* 4 (2013) 1446–1455.
- [11] C.Y. Chang, C.E. Wu, S.Y. Chen, C. Cui, Y.J. Cheng, C.S. Hsu, Y.L. Wang, Y. Li, *Angew. Chem.* 50 (2011) 9386–9390.
- [12] M. Biering, J.S. Nielsen, A. Siu, N.C. Nielsen, F.C. Krebs, *Sol. Energy Mater. Sol. Cells* 92 (2008) 772–784.
- [13] J. Mikroyannidis, D. Tsakournos, P. Balraju, G. Sharma, *J. Power Sources* 196 (2011) 2364–2372.
- [14] J.A. Hauch, P. Schilinsky, S.A. Choulis, R. Childers, M. Biele, C.J. Brabec, *Sol. Energy Mater. Sol. Cells* 92 (2008) 727–731.
- [15] B.J. Leever, C.A. Bailey, T.J. Marks, M.C. Hersam, M.F. Durstock, *Adv. Energy Mater.* 2 (2012) 120–128.
- [16] H.Z. Yu, J.B. Peng, *Org. Electron.* 9 (2008) 1022–1025.

- [17] M. Pfeiffer, A. Beyer, B. Plonnigs, A. Nollau, T. Fritz, K. Leo, D. Schlettwein, S. Hiller, D. Wohrle, *Sol. Energy Mater. Sol. Cells* 63 (2000) 83–99.
- [18] Y. Kim, S. Cook, S.A. Choulis, J. Nelson, J.R. Durrant, D.D.C. Bradley, *Chem. Mater.* 16 (2004) 4812–4818.
- [19] X. Gong, M. Tong, F.G. Brunetti, J. Seo, Y. Sun, D. Moses, F. Wudl, A.J. Heeger, *Adv. Mater.* 23 (2011) 2272–2277.
- [20] L. Li, W. Hu, H. Fuchs, L. Chi, *Adv. Energy Mater.* 1 (2011) 188–193.
- [21] M. Jørgensen, K. Norrman, F.C. Krebs, *Sol. Energy Mater. Sol. Cells* 92 (2008) 686–714.
- [22] S.A. Gevorgyan, M. Jørgensen, F.C. Krebs, *Sol. Energy Mater. Sol. Cells* 92 (2008) 736–745.
- [23] J. Peet, J.Y. Kim, N.E. Coates, W.L. Ma, D. Moses, A.J. Heeger, G.C. Bazan, *Nat. Mater.* 6 (2007) 497–500.
- [24] A.K. Pandey, M. Aljada, M. Velusamy, P.L. Burn, P. Meredith, *Adv. Mater.* 24 (2012) 1055–1061.
- [25] J.Y. Kim, S.H. Kim, H.H. Lee, K. Lee, W. Ma, X. Gong, A.J. Heeger, *Adv. Mater.* 18 (2006) 572–576.
- [26] J. Kim, H. Choi, C. Nahm, J. Moon, C. Kim, S. Nam, D.-R. Jung, B. Park, *J. Power Sources* 196 (2011) 10526–10531.
- [27] K. Walzer, B. Maennig, M. Pfeiffer, K. Leo, *Chem. Rev.* 107 (2007) 1233–1271.
- [28] J.B. Kim, Z.-L. Guan, A.L. Shu, A. Kahn, Y.-L. Loo, *Langmuir* 27 (2011) 11265–11271.
- [29] A. Martínez-Otero, X. Elias, R. Betancur, J. Martorell, *Adv. Opt. Mater.* 1 (2013) 37–42.
- [30] B.E. Lassiter, G. Wei, S. Wang, J.D. Zimmerman, V.V. Diev, M.E. Thompson, S.R. Forrest, *Appl. Phys. Lett.* 98 (2011) 243307–243309.
- [31] K.-M. Lee, W.-H. Chiu, M.-D. Lu, W.-F. Hsieh, *J. Power Sources* 196 (2011) 8897–8903.
- [32] J. Huang, J. Yu, H. Lin, Y. Jiang, *J. Appl. Phys.* 105 (2009) 073105–073109.
- [33] J.-P. Duan, P.-P. Sun, C.-H. Cheng, *Adv. Mater.* 15 (2003) 224–228.
- [34] B.W. D'Andrade, S.R. Forrest, *Adv. Mater.* 16 (2004) 1585–1595.
- [35] M. Tavakkoli, R. Ajeian, M.N. Badrabad, S.S. Ardestani, S.M.H. Feiz, K.E. Nasab, *Sol. Energy Mater. Sol. Cells* 95 (2011) 1964–1969.
- [36] A.J. Das, K.S. Narayan, *Adv. Mater.* 25 (2013) 2193–2199.
- [37] E. Voroshazi, B. Verreet, T. Aernouts, P. Heremans, *Sol. Energy Mater. Sol. Cells* 95 (2011) 1303–1307.
- [38] M.O. Reese, S.A. Gevorgyan, M. Jørgensen, E. Bundgaard, S.R. Kurtz, D.S. Ginley, D.C. Olson, M.T. Lloyd, P. Moryllo, E.A. Katz, A. Elschner, O. Haillant, T.R. Currier, V. Shrotriya, M. Hermenau, M. Riede, K.R. Kirov, G. Trimmel, T. Rath, O. Inganas, F. Zhang, M. Andersson, K. Tvingstedt, M. Lira-Cantu, D. Laird, C. McGuiness, S. Gowrisanker, M. Pannone, M. Xiao, J. Hauch, R. Steim, D.M. DeLongchamp, R. Roesch, H. Hoppe, N. Espinosa, A. Urbina, G. Yaman-Uzunoglu, J.-B. Bonekamp, A.J.J.M. van Breemen, C. Girotto, E. Voroshazi, F.C. Krebs, *Sol. Energy Mater. Sol. Cells* 95 (2011) 1253–1267.
- [39] J. Wagner, M. Gruber, A. Hinderhofer, A. Wilke, B. Broeker, J. Frisch, P. Amsalem, A. Vollmer, A. Opitz, N. Koch, F. Schreiber, W. Brütting, *Adv. Funct. Mater.* 20 (2010) 4295–4303.
- [40] J. Yuan, Z. Zhai, H. Dong, J. Li, Z. Jiang, Y. Li, W. Ma, *Adv. Funct. Mater.* 23 (2013) 885–892.